Preprints.org

Article

Riverine Particulate Material Enhances the Growth and Sustains the Viability of the Marine Diatom *Thalassiosira Weissflogii*

Christian Grimm , Agnes Feurtet-Mazel , Oleg Pokrovsky [*] , Erci Oelkers

Article

Riverine Particulate Material Enhances the Growth and Sustains the Viability of the Marine Diatom *Thalassiosira weissflogii*

Christian Grimm [1], **Agnès Feurtet-Mazel** [2], **Oleg S. Pokrovsky** [1,3,4,*] **and Eric H. Oelkers** [1,5]

[1] GET, CNRS/URM 5563, Université Paul-Sabatier, 14 avenue Edouard-Belin, 31400 Toulouse, France
[2] University of Bordeaux, CNRS, UMR EPOC 5805, Aquatic Ecotoxicology, Arcachon, France
[3] BIO-GEO-CLIM Laboratory, Tomsk State University, 36, Lenin avenue, 634050, Tomsk, Russia
[4] N. Laverov Federal Center of Integrated Arctic Research, Russian Academy of Science, Arkhangelsk, Russia
[5] Earth Sciences, University College London, Gower Street London WC1E 6BT, UK
[*] Correspondence: oleg@pokrovski.get.omp.eu

Abstract: Riverine particulates dominate the transport of vital nutrients like Si, Fe or P to the ocean margins, where they may increase primary production by acting as slow release fertilizer. Furthermore, the supply of particulate surface area to the ocean is considered to be a major control organic carbon burial. Taken together, these observations suggest a close link between the supply of riverine particulate material and the organic carbon cycle. To explore this link, we conducted microcosm experiments to measure the growth of the marine diatom *Thalassiosira weissflogii* in the presence and absence of different types and concentrations of riverine particulate material. Results demonstrate a strong positive effect of riverine particulate material on diatom growth with increased total diatom concentrations and slowed post-exponential death rates with increasing particulate concentration. Moreover, SEM and optical microscope investigations confirm that riverine particulates facilitates organic carbon burial through their role in the aggregation and sedimentation of phytoplankton. The supply of riverine particulate material has been shown to be markedly climate sensitive with their fluxes increasing dramatically with increasing global temperature and runoff. This pronounced climate sensitivity implies that riverine particulates contribute substantially in regulating atmospheric CO_2 concentrations through their role in the organic carbon cycle.

Keywords: riverine particulate material; phytoplankton; seawater; growth; organic carbon cycle; nutrients; primary production; carbon burial; CO_2

1. Introduction

The atmospheric concentration of carbon dioxide has been steadily increasing since the beginning of the industrial revolution and exhaustive evidence demonstrates its link to global climate change [1–3]. Over geological time, atmospheric CO_2 concentrations have been profoundly influenced 1) by oceanic primary productivity and the subsequent burial of organic matter [4–6], referred to as the 'biological pump' or the 'organic pathway' and 2) by weathering of Ca-Mg-silicates and the subsequent precipitation of carbonates, referred to as the 'inorganic pathway' [4,7–11]. Several studies have demonstrated a feedback between climate change and the inorganic pathway. This feedback stems from global air temperatures increasing in response to increasing atmospheric CO_2 concentrations, leading to changing precipitation patterns, increasing continental runoff and elevated chemical and physical weathering rates [12]. Increasing weathering rates drive CO_2 drawdown via through the delivery of divalent cations from silicate minerals and the subsequent precipitation of carbonates in the oceans [12–15]. This has been referred to as the internal thermostat of the Earth [7,9].

The effect of a changing climate on the global biological pump has been subject of numerous studies including the consequence of changing temperature and CO_2 partial pressure (pCO_2) on marine primary production [16–25]. Currently, the marine science community cannot confidently predict whether the biological pump will weaken or strengthen in a high CO_2 world [20,22,23,26–28].

The response of phytoplankton to environmental stress associated with climate change comprises not only elevated pCO_2, temperature and concomitant ocean acidification but also changing nutrient availabilities. The two major sources of nutrients to the ocean are the recycling of organic compounds and the influx of new nutrients through rivers, aeolian dust or volcanic ash [29–34]. Of the nutrients arriving from the continents, the riverine particulate input is the most important. Estimates suggest global land-to-ocean fluxes of 15-20 Gt year^{-1} for suspended riverine particulate material, 1.6-10 Gt year-1 for riverine bedload material, ~1 Gt year^{-1} for riverine dissolved load and ~0.4 Gt year-1 for aeolian dust [35–42]. Thus, the riverine particulate flux exceeds the dissolved flux by a factor of 17-30 and the aeolian dust flux by a factor of 40-75. Notably, due to their low solubility, the particulate flux of limiting nutrients like Si, P and Fe exceeds the corresponding dissolved flux by factors of 50, 100 and 350 [41,43]. Such observations suggest a major impact of riverine particulates on primary production in the global oceans. Jeandel and Oelkers [43] summarized the fate of riverine particulate material reaching the coastal ocean and highlight its role in the global cycle of the elements and its feedback on climate change through serving as slow release fertilizer for marine primary production.

Ocean water is largely depleted in dissolved silica and thus its availability limits primary production in various marine settings [44]. Diatoms account for 75 % of the primary productivity in high nutrient and coastal regions and 40 % of the total annual marine primary production [26,44–46]. About half the total global primary productivity occurs in the oceans, thus, diatoms contribute about 20 % of the annual total primary production that occurs on Earth [44,47]. Several recent studies have suggested that anthropogenic global change may alter greatly the marine diatom community affecting significantly the biological pump (e.g., ref. [46,48–53]).

To effectively remove CO_2 from the atmosphere via the organic pathway, organic carbon produced during photosynthesis needs to be transported down the water column to escape decomposition [4,9,43,54,55]. Thus, besides the net primary productivity, the export of atmospheric CO_2 via the organic pathway depends on the burial efficiency of organic matter, which is closely related to the formation of aggregates and their sedimentation capability [56–59]. A significant proportion of surface-derived organic matter sinks to the ocean floor as 'marine snow' (aggregates >500 μm), formed during phytoplankton blooms [57,58]. Marine snow can be formed biologically as fecal pellets through grazing and excretion or through physical aggregation [60], whereby physical aggregation explains the bulk of post-bloom particle aggregation [61,62]. The coagulation of small particles to larger aggregates scales with the square of particle concentration [61–63]. Hill [62] concluded in his coagulation model, that high particle concentrations and abundant non-phytoplankton particles are necessary to match the observed aggregation and sedimentation rates in the ocean [57]. Mineral particles have been found to promote particle coagulation through electrostatic forces or hydrogen bonds [64–68]. Furthermore, the incorporation of mineral particles with a high specific density into marine snow usually leads to higher sinking velocities [69,70], although the reverse effect might occur, due to the fragmentation of aggregates in the presence of mineral particles [71,72]. Liu et al. [73] demonstrated that the presence of suspended detrital clays in oceanic environments exerts a crucial control on the formation of co-aggregates between filamentous cyanobacteria and clay minerals and is thus important in the sedimentation and subsequent preservation of cyanobacteria. Diatoms are particularly efficient in transporting organic carbon from the surface water to the deep ocean by forming large aggregates with high settling velocities [23,61,74,75]. Notably, large sedimentation events are frequently dominated by diatoms due to their capability to form marine snow sized aggregates [23,28,57].

The supply of mineral particles to the ocean is predicted to change significantly with climate change [12,15,68] but the specific details and consequences of this change are still unclear. Gislason et al. [12] observed that the riverine particulate flux is far more climate sensitive compared to the

corresponding dissolved flux. The potential influence of a changing particulate flux to the oceans on the biological pump are expected to have global consequences because riverine particulates 1) deliver limiting nutrients, thus increasing marine primary production and 2) increase organic carbon burial rates due to the strong organic material sorption onto mineral surfaces [71,76]. However, experimental calibration of the effect of river suspended material on growth of coastal primary producers and related carbon sequestration remains limited.

This study aims to explore the effect of riverine particulate material on the growth of marine diatoms. Towards this goal, we conducted growth experiments with the marine diatom *Thalassiosira weissflogii* in the presence of different types and concentrations of riverine particulate material. We hypothesize that the presence of particulate matter may 1) accelerate the cell growth by providing nutrients and 2) scavenge cell exo-metabolites via adsorption on the particulate surfaces. The purpose of this paper is to verify these hypotheses and to discuss the potential role of riverine particulate material on the organic carbon cycle.

2. Materials and Methods

In this study, we performed microcosm experiments, investigating the growth of the marine diatom *Thalassiosira weissflogii* in the presence and absence of different types and concentrations of riverine particulate material to characterize the effect of riverine particulates on diatom productivity.

2.1. Riverine Particulate Material

Two types of riverine particulate material with distinct mineralogical and chemical compositions were used. The bulk chemical compositions, as well as the BET surface areas of these particulates are listed in Table 1 and consist of:

1) Mississippi (MS) bedload material collected in autumn 2015 in New Orleans near to the Department of Earth and Environmental Science of Tulane University. Due to the low water level in autumn 2015, the mud sample was collected from the usually flooded river bed. The sample consists of roughly 80 % SiO_2 and is mainly composed of quartz, and feldspars with minor quantities of sheet silicates. It was chosen as a representative of continental riverine material.

2) Iceland (ICE) suspended particulates collected from Jökulsá á Dal at Brú, a glacial river in Eastern Iceland. The ICE riverine particulate material mainly consists of basaltic glass and crystalline basalt fragments. This sample is representative of the high relief, volcanic and tectonic active islands that contribute over 45 % of river suspended material to the oceans [78,79]. Details on sampling and filtration methods can be found in ref. [78], where the chemical composition is provided (sample ID 01A034 therein).

Table 1. Whole rock analyses and specific surface areas of the Mississippi (MS) and Iceland (ICE) riverine particulate material used in this study. ICE data is from Eiriksdottir et al. (2008). Note that total Fe is presented as FeO or Fe_2O_3, respectively, for the ICE and MS samples.

Name	ICE	MS
Type	suspended	bedload
BET (m^2/g)	36.83	16.27
SiO_2 (%)	51.87	77.65
Na_2O (%)	2.22	1.20
MgO (%)	6.00	0.91
Al_2O_3 (%)	13.87	9.55
P_2O_5 (%)	0.24	0.14
K_2O (%)	0.40	1.70

CaO (%)	10.15	1.67
TiO_2 (%)	2.42	0.58
MnO (%)	0.21	0.09
FeO (%)	12.49	
Fe_2O_3 (%)		2.60
LOI		3.78

2.2. Datoms

The marine planktonic diatom *Thalassiosira weissflogii* (TW) used in this study was cultured under sterile conditions in Guillard´s f/2 enriched Instant Ocean© artificial seawater in a thermo-regulated growth chamber at the EPOC laboratory, University of Bordeaux in Arcachon. The chemical composition of the Instant Ocean© sea salt and the modified Guillard´s f/2 culture medium [80] used in the culture are provided in Table 2 and 3, respectively. *Thalassiosira weissflogii* is a common unicellular, bloom-forming diatom found in marine, estuarine and freshwater environments. It forms 4-32 μm diameter cylindrical silica valves [81] which occur as single cells or in groups. Due to its large mean size (~10 μm) TW is commonly used to feed shrimps and oysters. Further details about this diatom are provided in previous publications [44,46,82–86].

(Armbrust, 2009; De La Rocha and Passow, 2004; De La Rocha et al., 2010 Johansen and Theriot 1987, Roberts et al. 1997; Sorhannus et al. 2010; Vella et al., 2019).

Table 2. Elemental composition of Instant Ocean (IO) and natural surface seawater (SW) – after ref. [82].

	IO	SW
Major cations (mmol/kg)		
Na	462	470
K	9.4	10.2
Mg	52	53
Ca	9.4	10.3
Sr	0.19	0.09
Major anions (mmol/kg)		
Cl	550	550
SO_4	23	28
Trace elements (μmol/kg)		
Li	54	20
Si	16	5
Mo	1.8	0.1
Ba	0.85	0.04
V	2.95	0.04
Ni	1.7	0.004
Cr	7.5	0.003
Al	240	0.002
Cu	1.8	0.001
Zn	0.5	0.001

Mn	1.2	0.0004
Fe	0.24	0.0001
Cd	0.24	0.0001
Pb	2.1	0.00006
Co	1.3	0.00005
Ag	2.3	0.00001
Ti	0.67	0.00001

Table 3. Nutrient concentrations of modified pure and 5 % Guillard´s f/2 culture medium [80]. Note that no additional silica was added to the reactors except for the Si present in the Instant Ocean© as described in Table 2.

	pure f/2	5 % f/2
	(mmol/kg)	
$NaNO_3$	8.82×10^{-01}	4.41×10^{-02}
NaH_2PO_4	3.62×10^{-02}	1.81×10^{-03}
$FeCl_3$	1.17×10^{-02}	5.83×10^{-04}
$CuSO_4$	3.92×10^{-02}	1.96×10^{-03}
Na_2MoO_4	2.60×10^{-02}	1.30×10^{-03}
$CoSO_4$	3.56×10^{-02}	1.78×10^{-03}
$MnCl_2$	9.10×10^{-02}	4.55×10^{-03}
thiamine HCl (V B1)	2.96×10^{-04}	1.48×10^{-05}
biotine (V H)	2.05×10^{-06}	1.03×10^{-07}
cyanocobalamin (V B12)	3.69×10^{-07}	1.85×10^{-08}

2.3. Growth experiments

Inoculation experiments were performed in sterile 250 or 500 ml Polycarbonate flasks with 12 h/12 h illumination/dark cycles (3000 LUX cool white fluorescence light during daytime), circular shaking at 250 1/min, and room temperature. The polycarbonate flasks were closed with BIO-SILICO© N stoppers that allowed the sterile equilibration of the microcosms with the atmosphere. The reactive fluids were composed of either pure Instant Ocean© (IO) artificial sea salt solution or Instant Ocean© artificial seawater enriched with 5 % modified Guillard´s f/2 culture medium. One experimental series was performed in seawater enriched with 100 % Guillard´s f/2 culture medium. Note that no additional silica was added to the reactors except for the Si present in the Instant Ocean© sea salt solution. The chemical composition of Instant Ocean© and natural seawater are provided in Table 2, and the nutrient concentrations of pure and 5 % modified Guillard´s f/2 culture medium are given in Table 3. Salinities and pH were initially between 32-34‰ and 8.1-8.4 in each reactor. The riverine particulate material was cleaned with ethanol and flushed 3 times with deionized water and subsequently sterilized for >12h in the oven at 121°C. Prior to their use in the experiments. Particulates were added to the reactors in concentrations of 75, 100, 250, 500 and 750 mg/kg. Biotic controls without particulates and abiotic controls with particulates, but without bacteria, were run as part of each experimental series. All reactive fluids, as well as the experimental equipment were either filter-sterilized or autoclaved at 121 °C for 20 minutes prior to the experiment.

Aliquots of the diatoms were harvested from the stock solutions and rinsed three times in the experimental electrolyte solution by centrifugation/resuspension cycles prior to inoculation. Diatoms were inoculated at a concentration of ~104 cells/ml. All experiments were run in triplicate.

2.4. Sampling and analytical methods

Three ml aliquots of homogenous samples containing both the fluids and solids were periodically taken from each experiment in a sterile laminar hood box 6h after the onset of illumination; all solids were thoroughly resuspended prior to sampling. Cell density and pH measurements were performed immediately after sampling in the collected suspension samples. Solids were sampled after selected experiments and prepared for SEM analysis.

Cell densities were determined using a Nageotte counting chamber (grid of 40 fields of 1.25 μl each, 0.5 mm depth). Suspension samples were diluted prior to counting to attain a range of 10-100 cells per Nageotte field. To obtain accurate cell concentrations, 10 fields were counted for each sample. The pH was measured using a VWR semi-micro electrode with an uncertainty of ±0.05. To fit of the temporal evolution of the diatom concentration we applied [87]:

$$y = \frac{a}{1 + e^{-k(t-c)}} + a_0 \tag{1}$$

where *a* represents the upper asymptote of the sigmoidal growth curve, a_0 reflects the initial diatom concentration, *k* is a rate parameter describing the initial growth and *c* designates a time constant describing the time elapsed between the beginning of the experiment and the turning point (the point of maximal increase in diatom concentration). Sampled solids were characterized by scanning microscopy using a Jeol JSM 6360LV at the Laboratoire Géoscience Environnement Toulouse.

3. Results

A total of 5 experimental series were conducted, three in nutrient enriched artificial seawater solution (series TW1, TW2, and TW4) and two in artificial seawater without added dissolved nutrients (series TW3 and TW5). Table S1 of the Supplement summarizes the experimental conditions as well as the observed temporal evolution of diatom concentrations and pH during all experimental series.

3.1. Temporal evolution of diatom concentrations in experiments carried out in nutrient enriched Instant Ocean© - Experiments TW1, TW2, and TW4

Figure 1 shows the temporal evolution of the diatom concentration and pH in experimental series TW1 performed in Guillard′s f/2 enriched (100 % f/2 nutrient concentrations) Instant Ocean©, and in the presence and absence of 500 mg/kg MS and ICE riverine particulates. All diatom cultures exhibited exponential growth until the end of the experiment. Experiments were stopped before the cultures reached the stationary growth stage. Notably, initial diatom growth occurred earlier in the presence of riverine particulates compared to the biotic control and the final diatom concentration was 1.21±0.05 times greater in the presence of 500 mg/kg ICE particulates compared to the biotic control. The experiment performed in the presence of 500 mg/kg MS particulates showed a similar final diatom concentration as the biotic control. The pH in the biotic experiments (Figure 1B) increased from initially ~8.2 to 9.2-9.4. This >1 pH unit increase results from diatom photosynthetic activity. As carbon accumulates in the cells, HCO_3^- is converted by the enzyme carbonic anhydrase to CO_2, producing one mole of OH^- per mole of carbon [83]. The pH in the abiotic control experiments increased during the first 2 days slightly from ~8.2 to ~8.4 and remained constant until the end of these experiments.
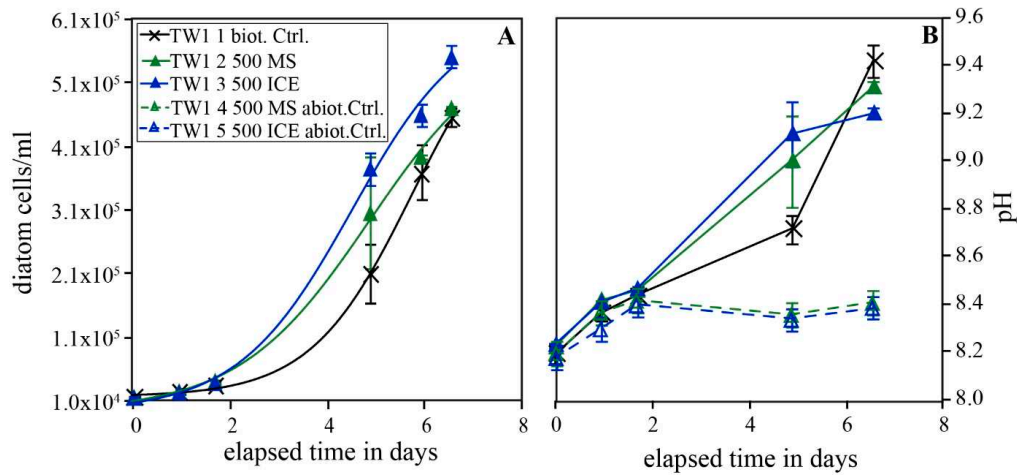
Figure 1. Temporal evolution of diatom concentration (A) and pH (B) during experimental series TW1 carried out Instant Ocean enriched with pure Guillard´s f/2 culture medium. The error bars represent the standard deviation of the triplicates.
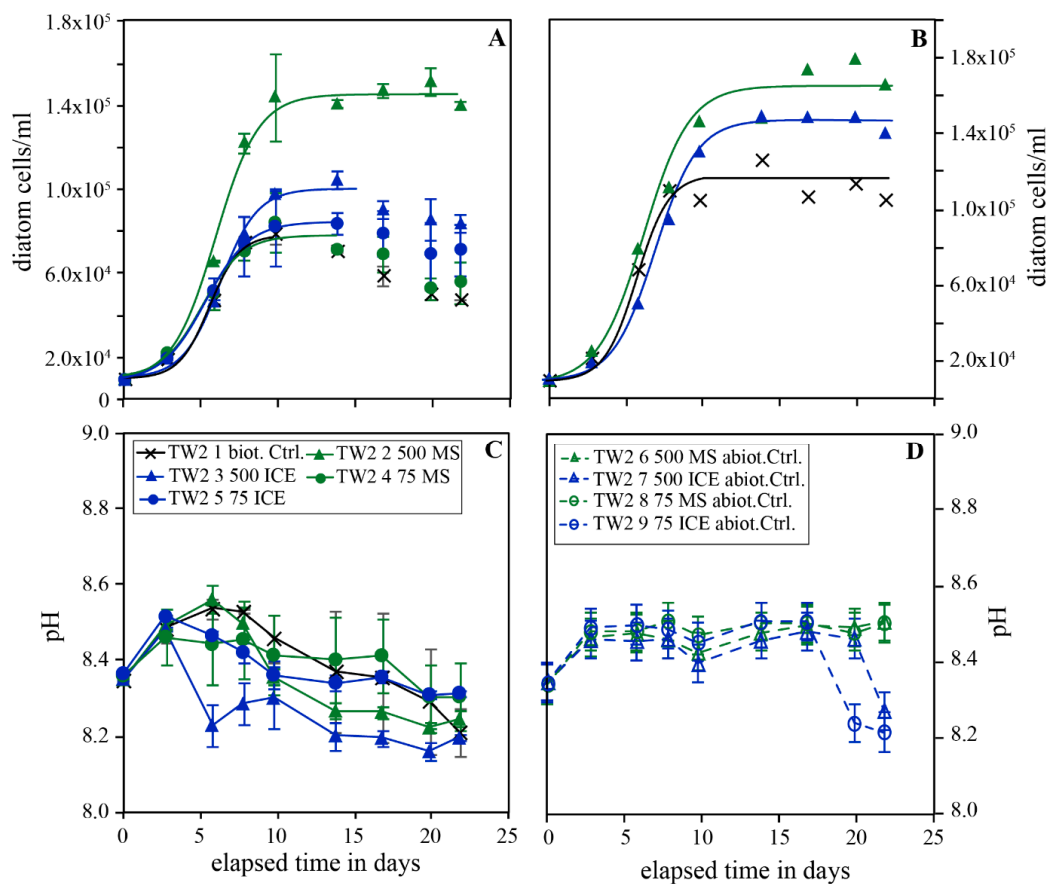

Figure 2. Temporal evolution of diatom concentration (A, B) and pH (C,D) in experimental series TW2 carried out in Instant Ocean© enriched with 5 % Guillard´s f/2 culture medium. Figure A shows the evolution of diatom concentration of experiments performed in 250 ml reactors, whereas Figure B shows the evolution in experiments performed in 500 ml reactors. Figure C shows the pH evolution of the biotic experiments and Figure D the pH evolution of the abiotic experiments. The error bars in A represent the standard deviation of the duplicates, in C and D of the triplicates. The uncertainty in diatom concentrations in Figure C is estimated to be below 10 %.

Figure 2 shows the temporal evolution of diatom concentration and pH in experimental series TW2 performed in Instant Ocean© artificial seawater solution enriched with 5 % Guillard´s f/2 culture medium, and in the presence and absence of 75 and 500 mg/kg MS and ICE riverine particulates. All biotic experiments showed typical logistic growth, however, distinct differences were observed depending on the presence or absence of riverine particulate material. Note, that for the biotic control and the experiments performed in the presence of 500 mg/kg MS and ICE particulates, two of the triplicates were conducted in 250 ml flasks and one in a 500 ml flask. Since the diatoms in the larger reactors showed notably more pronounced growth, they are illustrated separately (Figure 2A and C for the smaller reactors, Figure 2B and D for the larger reactors). Diatoms grew exponentially from the onset of the experiments for ~10 days when they reached the stationary phase. In the 500 ml reactors (Figure 2B), diatom concentrations remained constant after the exponential growth until the end of the experiment. In the 250 ml reactors, diatom concentrations remained constant after exponential growth only in the presence of 500 mg/kg MS particulates and decreased in all other experiments. The maximum diatom concentrations determined for each series in the small reactors increased by factors of 1.07 ± 0.18 and 1.06 ± 0.09 with the addition of 75 mg/kg MS and ICE particulates but by factors of 1.92 ± 0.08 and 1.32 ± 0.08 with the addition of 500 mg/kg MS and ICE particulates relative to the biotic control. In the 500 ml reactors, the presence of 500 mg/kg MS and ICE particulates resulted in an 1.42 ± 0.07 and 1.18 ± 0.07 times higher maximum diatom concentration relative to the biotic control without particulates. The pH in the biotic experiments increased slightly during the first 3-5 days from 8.35 to 8.5-8.6 and subsequently decreased to 8.2-8.3. Notably, pH in the biotic reactors doped with 500 mg/kg ICE particulates attained the final pH of 8.2-8.3 after only 5 days following a rapid decrease from 8.5 to 8.2. The pH in the abiotic controls increased during the first 3 days from 8.35 to 8.4-8.5 whereas it remained constant for reactors doped with MS particulates. In contrast, the pH dropped from 8.5 to 8.2 towards the end of the experiment in abiotic controls doped with ICE particulates.

Figure 3 shows the temporal evolution of TW concentration and pH during experimental series TW4 performed in Instant Ocean© enriched with 5 % Guillard´s f/2 culture medium, and in the presence and absence of 250 and 750 mg/kg MS and ICE riverine particulates. All TW cultures showed exponential growth from the onset of the experiment until day 12-15 when the cultures attained the stationary phase and cell concentrations started to decrease in all reactors. This post-exponential decay was most pronounced in the biotic control experiment without particulates. In the presence of 750 mg/kg ICE particulates, growth occurred, but lagged by 3-4 days. The measured maximum diatom concentration increased by factors of 1.10 ± 0.07 and 1.27 ± 0.08 in the presence of 250 and 750 mg/kg MS particulates and slightly by factors of 1.08 ± 0.09 and 1.04 ± 0.13 in the presence of 250 and 750 mg/kg ICE particulates relative to the biotic control. The pH in the biotic experiments doped with MS particulates increased initially from 8.45 to 8.6, then decreased to 8.3 and remained constant during the last 8 days of experiment. In the biotic control and the reactors doped with ICE particulates, pH decreased during the first 3 days from 8.45 to 8.3-8.4 and 8.2-8.3, then it remained constant. The pH in the abiotic controls doped with MS particulates increased slightly from 8.45 to 8.55 during the course of the experiment. In abiotic controls doped with ICE particulates, pH remained constant at ~8.45 for the first 10 days but then decreased to 8.2 towards the end of the experiment.
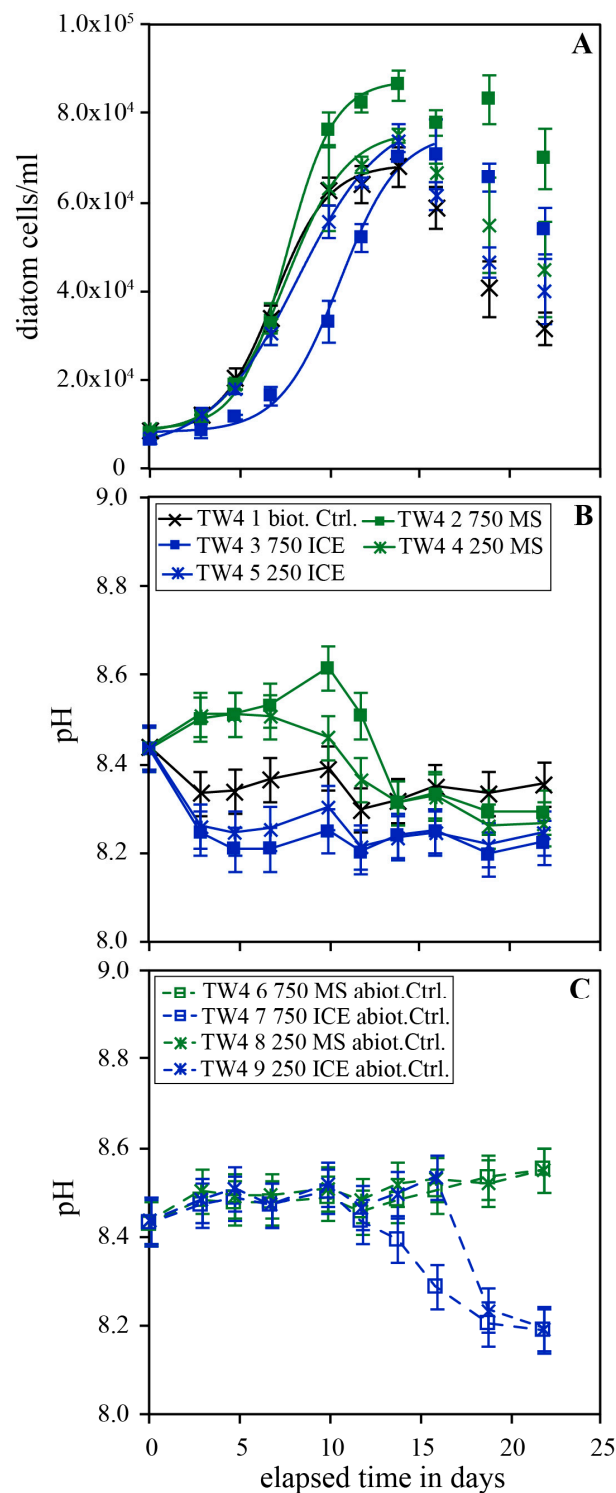
Figure 3. Temporal evolution of diatom concentration (A), pH (B) and pH in the abiotic control (C) of experimental series TW4. The error bars represent the standard deviation of the triplicates.

3.2. Temporal evolution of diatom concentrations in Instant Ocean© without added dissolved nutrients - Experiments TW3 and TW5.

In experiments conducted in Instant Ocean© without additional nutrients, diatom cultures did not exhibit an exponential growth stage. However, a pronounced positive effect of riverine particulates on diatom growth was observed in these experiments.

Figure 4 shows the temporal evolution of diatom concentration and pH in experimental series TW3 performed in Instant Ocean© in the presence and absence of 100 and 500 mg/kg MS and ICE riverine particulates. The initial diatom concentration was identical in all reactors since the solutions were all derived from the same dilution of the original culture. Thus, the observed lower concentration at the onset of the experiments doped with particulates is likely an artifact resulting from the increased turbidity and a concomitant underestimation of diatom concentration due to a more difficult traceability of the diatoms in the counting chamber. This is particularly evident for the more fine-grained ICE particulates. Diatom concentrations in the biotic control continuously decreased during the experiments. In the presence of 500 mg/kg MS particulates, diatom concentrations increased linearly from day 3 to 20 of the experiment resulting in a 13.55 ± 0.31 times greater final diatom concentration compared to the biotic control. In the presence of 500 mg/kg ICE particulates, this linear growth was less pronounced but diatoms likewise grew during day 3 to 20 resulting in a 6.30 ± 0.26 times greater final diatom concentration compared to the biotic control. Continuous growth was not observed in reactors doped with 100 mg/kg MS or ICE particulates but diatom concentrations notably decreased less rapidly compared to the biotic control, resulting in 3.86 ± 0.31 and 2.16 ± 0.32 times greater final diatom concentrations, respectively. The pH evolution was similar as in previously described experiments with a constant or slightly increasing pH in reactors doped with MS particulates and a decrease in pH by ~0.2 pH units in reactors doped with ICE particulates.

Figure 5 shows the temporal evolution of diatom concentration and pH in experimental series TW5 performed in Instant Ocean© in the presence and absence of 250 and 750 mg/kg MS and ICE riverine particulates. Similar as shown in Figure 4, diatom concentrations in the biotic control experiments continuously decreased during the experiments. In the presence of 750 mg/kg MS particulates, however, diatom concentration increased linearly throughout the experiment. In experiments doped with 250 mg/kg MS or ICE, and 750 mg/kg ICE particulates, diatom concentrations increased during days 1-9 and 1-15 of the experiment, respectively. This resulted in final diatom concentrations 7.87 ± 0.16 and 4.25 ± 0.17 times greater than the biotic control in the presence of 750 mg/kg MS and ICE particulates, respectively. With the addition of 250 mg/kg MS and ICE particulates, the final diatom concentrations increased by factors of 2.87 ± 0.17 and 1.20 ± 0.20 relative to the biotic control. The pH remained constant at 8.3-8.4 after an initial increase from 8.1 in all biotic and abiotic reactors.
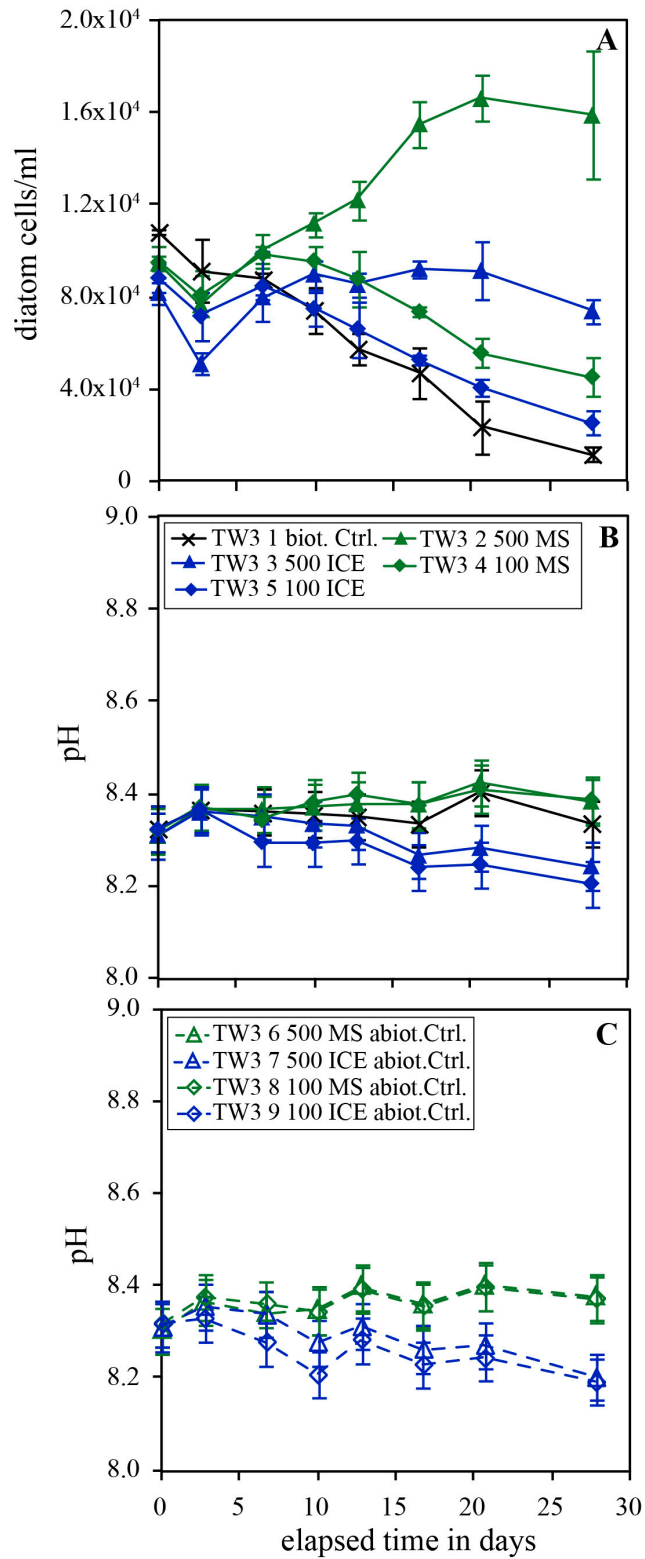
Figure 4. Temporal evolution of diatom concentration (A), pH (B) and pH in the abiotic control (C) of experimental series TW3 carried out in Instant Ocean without additional nutrients. The error bars represent the standard deviation of the triplicates.
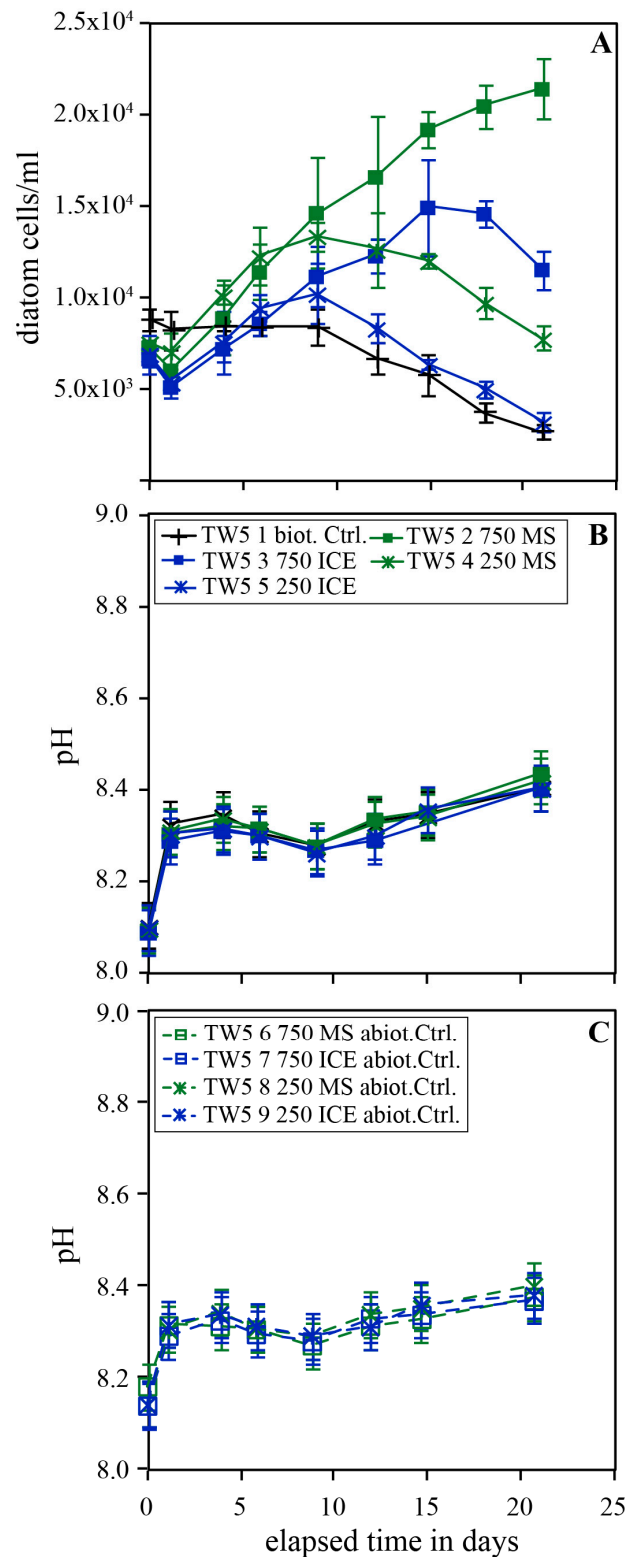
Figure 5. Temporal evolution of diatom concentration (A), pH (B) and the pH in the abiotic control (C) of experimental series TW5 carried out in Instant Ocean without additional nutrients. The error bars represent the standard deviation of the triplicates.

3.3. SEM and optical microscopy

During cell counting using the optical microscope, diatoms were frequently found agglomerated in groups of about 10-50 cells mingled with sediment particles. This was evident for all experiments performed in the presence of MS and ICE particulates. This observation was confirmed by SEM

investigations (see Figure 6) showing agglomerates of diatoms and sediment particles, which appear to be held together with organic substances (Figure 6C).
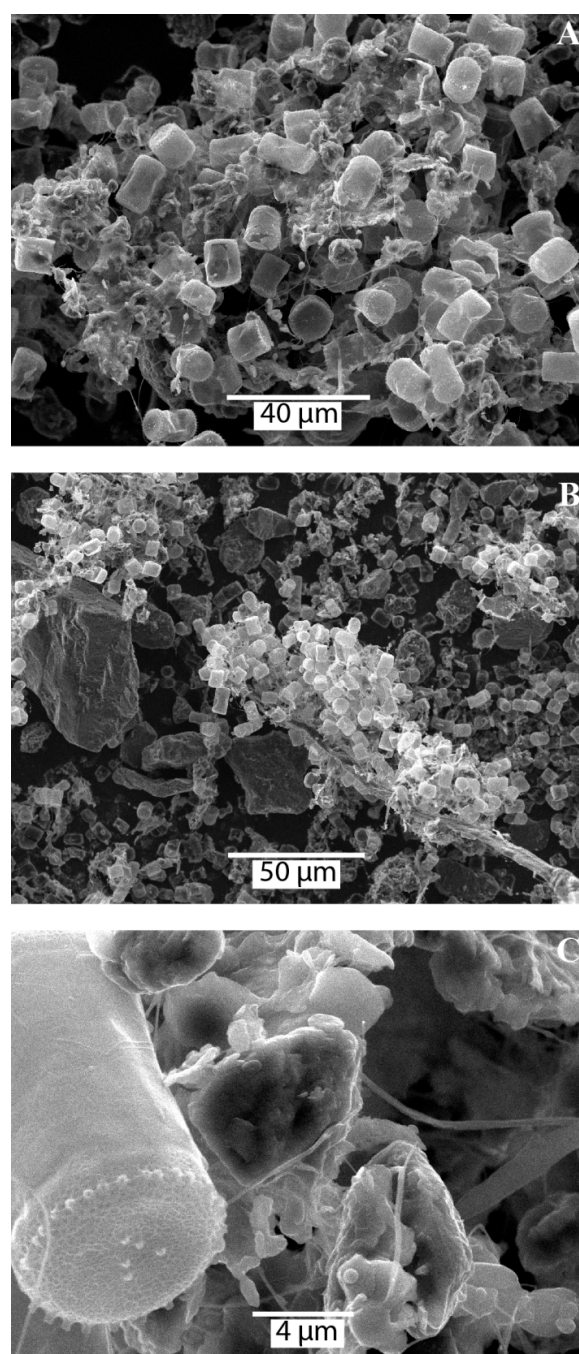

Figure 6. SEM photographs of experiment TW2 2-R1 performed in 5 % f/2 enriched artificial seawater in the presence of 500 mg/kg MS particulates. Diatoms were frequently found agglomerated with sediments, glued by organic substances.

4. Discussion

4.1. Summary of the effect of MS and ICE riverine particulate material on diatom growth

The microcosm growth experiments performed in this study can be subdivided into two categories with different initial conditions: a) series TW1, TW2 and TW4 were performed in nutrient enriched artificial seawater and b) series TW3 and TW5 were performed in artificial seawater without additional nutrients. In both initial conditions, the presence of riverine particulate material increased diatom growth or maintained their viability.

The effect of riverine particulate material on the growth of diatom in nutrient enriched artificial seawater is summarized in 7, which shows the maximum (TW_{max}) and final (TW_{final}) diatom concentrations as a function of MS (Figure 7A) and ICE (Figure 7B) particulate concentrations. Throughout all experiments, the maximum and final diatom concentrations increased with increasing particulate concentration. However, this effect was more pronounced in the presence of MS compared to ICE particulates. Furthermore, the post-exponential decrease from the maximum diatom concentrations (TW_{max}) to the final concentration (TW_{final}) was distinctly less pronounced in experiments performed in the presence of riverine particulates compared to the biotic controls. This is evidenced by the steeper slope of the regression lines of the TW_{final} compared to the TW_{max} concentrations and the resulting convergence of the two linear fit lines shown in 7A and B.
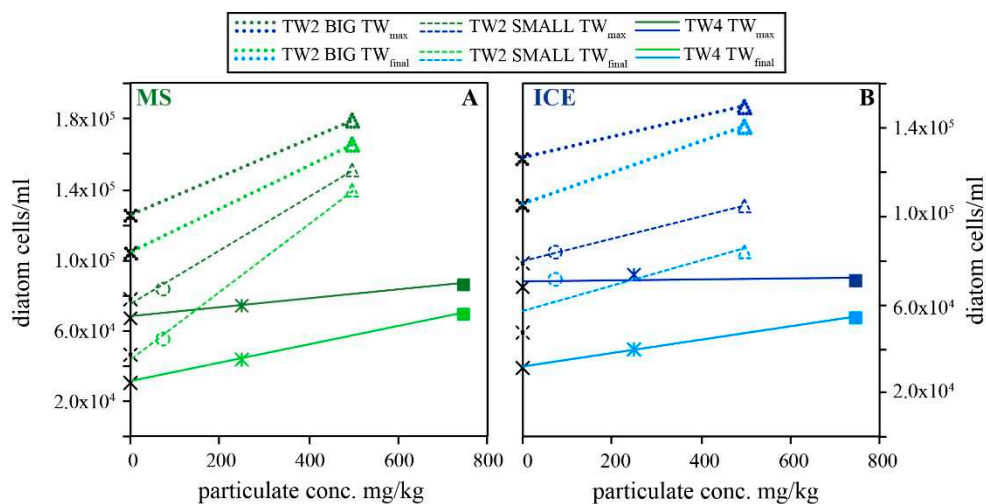

Figure 7. Measured maximum (TWmax) and final (TWfinal) diatom concentrations as a function of MS (A) and ICE (B) riverine particulate concentration for experimental series TW2 and TW4 performed in Instant Ocean enriched with 5% Guillard´s f/2 culture medium. BIG and SMALL refers to the 500 ml and 250 ml reactors used in series TW2. Biotic controls without particulates are indicated as black crosses on the y-axes. Increasing particulate concentration raised diatom concentrations compared to the biotic control without particulates.

The effect of riverine particulate material on the diatom growth in artificial seawater without nutrient enrichment is summarized in Figure 8, which shows the temporal evolution of diatom concentrations in the presence of MS particulates (Figure 8A), in the presence of ICE particulates (Figure 8B) and the biotic controls in the absence of added particulates (Figure 8C) during the first 13 days of each experiment. In all biotic controls, diatom concentrations continuously decreased during the experiments, whereas continuous growth was observed in experiments doped with ≥100 mg/kg MS and ICE particulates. In the presence of 100 mg/kg MS and ICE particulates, diatom concentrations stayed close to constant or decreased slightly but less rapidly than in the biotic controls, resulting in higher final diatom concentrations.
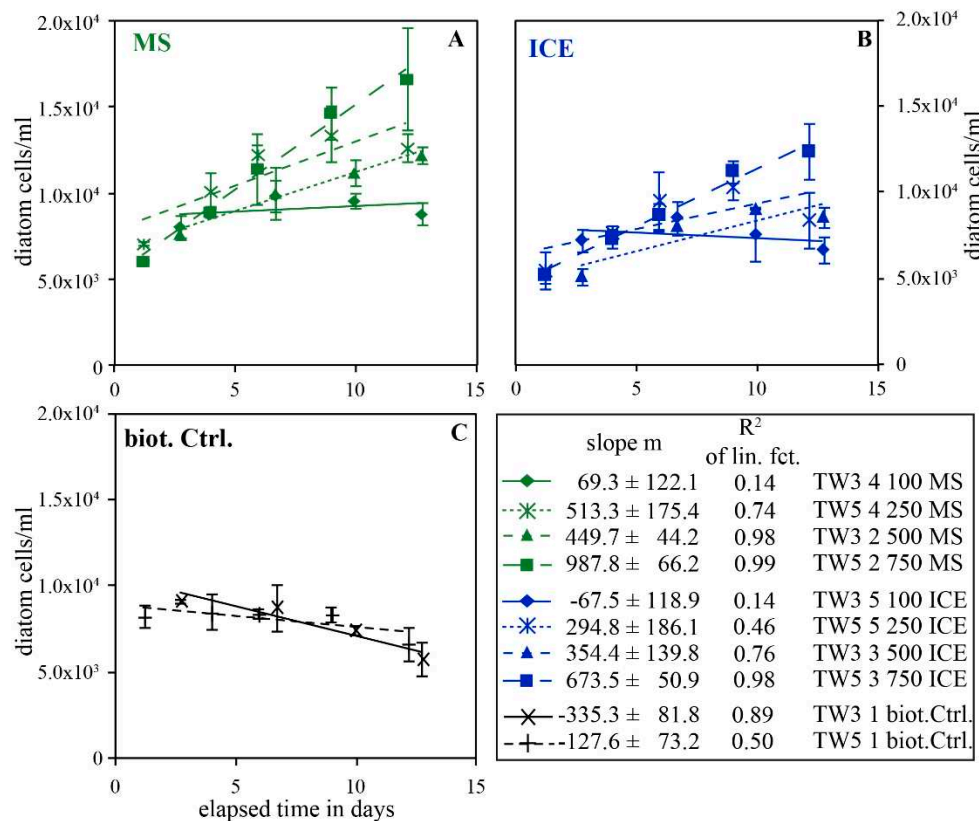
Figure 8. Temporal evolution of diatom concentration during the first 13 days of experimental series TW3 and TW5, performed in Instant Ocean without additional nutrient enrichment. A and B show results from experiments performed in the presence of MS and ICE particulates and C shows results of the biotic controls without particulates. Lines show linear best fits of the data, the slopes of these fits are provided in the lower right box. The presence of particulates caused a linear diatom growth, whereas diatom numbers decreased with time in the biotic controls without particulates.

The linear growth observed during the experiments containing ≥100 mg/kg particulates is highlighted in Figure 9 which shows the slope of the best linear fits given in 8, as a function of MS and ICE particulate concentrations added to the reactors. To a first approximation, these data are linear functions of particulate concentration, and consistent with rates of 1.42 ± 0.31 ($R^2 = 0.87$) and 1.13 ± 0.18 ($R^2 = 0.92$) diatom cells/ml/day per mg/kg MS and ICE particulate material, respectively. With a diatom (TW) cell organic carbon content of about 30-180 pg C/cell [44,84,88], this corresponds to organic carbon formation rates ranging from 43 ± 9 to 255 ± 57 and 34 ± 6 to 203 ± 33 pg C/ml/day per each mg/kg MS and ICE particulate material, respectively. This estimate takes into account only cellular organic carbon and thus excluded extracellular C_{org}, which may significantly contribute to the total organic carbon content. Similar to the experiments performed in nutrient enriched Instant Ocean©, MS particulates showed a greater effect on diatom growth than ICE particulates.

During this study, growth experiments were performed using only one single species of phytoplankton, the diatom *Thalassiosira weissflogii*. The two types of riverine particulate material used in the study cover a wide range of chemical compositions (silicic to basaltic). The basaltic sediment from Iceland might be expected to have a greater effect on diatom growth due to the more rapid release of silica, the main constituent of the diatom frustules [89–91].
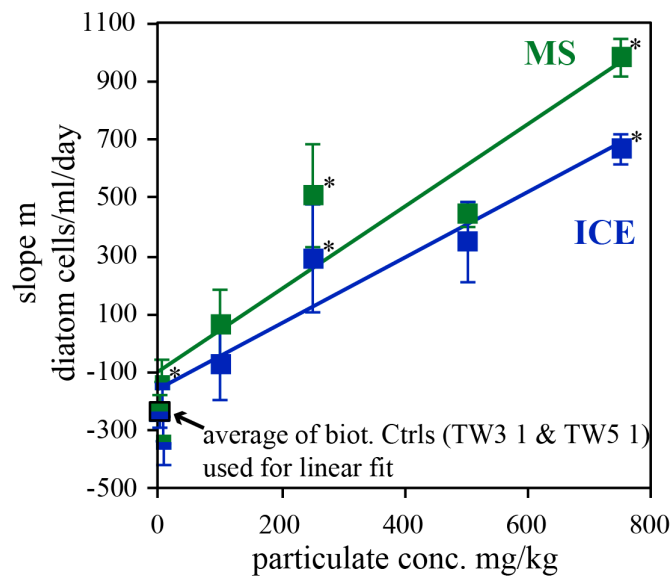
Figure 9. Slope of the linear best fits given in Figure 8 plotted against the particulate concentration added to the reactors. Data points with a star (*) represent results of experimental series TW3, those without a star are from series TW5. Solid lines represent linear best fits of the data, whereby the average of the two biotic controls at 0 mg/kg particulates was used. Error bars reflect the uncertainty of the slope (see box in Figure 8).

However, Mississippi particulates showed a more pronounced effect on diatom growth compared to Iceland particulates in all experimental series. Thus, the observed positive effect of particulate material on phytoplankton growth may be due to the presence of certain mineral phases, such as clays, or the presence of highly reactive nanoparticles adhering to larger grains [92]. Furthermore, we suggest that the stronger effect of MS particulates compared to ICE particulates might stem from a higher concentration of adsorbed macro- and micronutrients on the surfaces of the Mississippi River sediments, impacted by anthropogenic and agricultural activity. Abiotic experiments of nutrient desorption from riverine particulate material would be necessary to quantify this difference. The role of physical contact between particulate material and algae may also play a role. For example, some phytoplankton have cell-surface enzymes that could control this contact nutrient transfer (e.g., ref. 93).

The observation that silica release rates from sediments may not be the most important factor limiting diatom growth rates suggests that the release of nutrients from riverine particulates may be critical to the primary productivity in natural waters. As such, it seems likely that the presence of particles will positively affect the growth of other primary producers, which do not depend on silica, such as cyanobacteria, the oldest known organisms on Earth. Thus, riverine particulates might be expected to affect global primary production and consequently global biogeochemical cycles of several elements, today and in the past.

4.2. Potential role of riverine particulate material in natural systems

Jeandel and Oelkers [43] concluded that riverine particulate material dissolution in seawater has a large influence on ocean chemistry and the global cycle of the elements. Therein, Jeandel and Oelkers highlighted the potential role of riverine particulate material as slow release fertilizer supporting oceanic primary productivity and organic carbon burial. The results obtained in this study demonstrate that riverine particulates can enhance diatom growth in seawater and thus validate the influence of terrigenous sediments on marine primary productivity. This possibility is also supported the strong positive correlation observed between continental weathering rates and the abundance of diatoms in the oceans [94].

Diatom blooms commonly occur during spring and early summer when light availability maximizes, seawater temperatures rise and ocean water stratification is favorable. In the Arctic and

subarctic, this coincides with the peak of the suspended material delivery by the rivers to the ocean during freshet [95–97]. Moreover, Gislason et al. [15] observed that the maximum particulate fluxes in rivers in NE Iceland occur during the spring when ice melting maximizes. Thus, in times of highest oceanic primary productivity, riverine particulate fluxes from the continents to the oceans also maximize suggesting an important role of these particulates in delivering limiting nutrients including silica. Moreover, at this time during the year, the less particulate dense and thus nutrient-rich river water floats on top of the denser seawater, creating a surface layer favorable for primary production. The potential effect of riverine particulates on primary production, however, depends on the environment. Wherever nutrients limit phytoplankton growth, riverine particulates could be expected to increase growth due to the nutrient delivery. Evidence for this can be found following the damming of rivers. Dam construction reduces sediment arrival to estuarine ecosystems. This can have a major impact on primary productivity. For example, Baisre and Arboleya [98] described a reduction in nutrient concentrations resulting from decreasing suspended sediment input in a Cuban estuary, which had a profound negative influence on the local ecosystem and on the regional fish industry. Suspended particulates, however, can also reduce light transmittance in the water column, which can decrease primary production if growth is light limited. This process can lead to observation that primary productivity is inversely related to the suspended particulate concentration in marine systems (e.g. [99]). For example, Jiang et al. [100] and Chen et al. [101] observed increasing chlorophyll a concentrations with decreasing suspended sediment input in Chinese estuaries, as a consequence of dam constructions. Note, however, these studies also report a concurrent increased occurrence of harmful algae blooms in these estuaries.

The large input of anthropogenic dissolved phosphate and nitrogen from agricultural use to coastal waters is known the increase eutrophication, potentially causing harmful algae blooms. Riverine particulates, however, release nutrients through mineral dissolution. The consumption of nutrients from seawater lowers the degree of saturation of nutrient-bearing minerals, thereby enhancing their release by accelerating mineral dissolution. In this way, particulates act as slow release fertilizer providing nutrients for phytoplankton growth in a buffered manner. Furthermore, particulates oppose harmful algal blooms through their ability to form sediment/algal flocs, which sink rapidly in the water column [66]. As shown in Figure 6, the diatoms in this study agglomerated into larger groups when particulates were present in the reactors. Such observations, commonly reported in the literature verifies the effect of riverine particulates on organic carbon burial since larger agglomerates have greater settling velocities than single diatom cells (e.g. [102–104]). Such observations supports the 'ballast hypothesis' (e.g. [105,106]), which proposes that mineral fragments increase organic carbon burial due to the formation of fast-settling mineral-phytoplankton aggregates.

Phytoplankton is known to have developed powerful strategies to gain access to vital nutrients. For example, bacteria and blue-green algae release siderophores with a high affinity for iron, which are recognized by receptor sites on the cell surface and transported across the cell membrane [107]. Similarly, chelators are known to depress toxic metal activity or to increase ferric oxide solubility making Fe bio-available [107,108]. Furthermore, depending on the mechanism of carbon uptake, phytoplankton may alter the surrounding fluid pH [108,109], which can increase nutrient availability through enhanced mineral dissolution in the cell microenvironment [108,110]. Direct and indirect interactions of microbes and inorganic substances are omnipresent in natural systems and several studies have demonstrated the ability of microbes to acquire nutrients directly from minerals [111–114]. It is generally believed that most nutrient transfer between suspended particulate material and phytoplankton occurs indirectly, and rely on both desorption and release from deposited sediments and mixing upwards into the photic zone [115]. Riverine particles can release elements to the oceans by desorption, exchange or dissolution [116–118]; several examples are summarized in Jeandel and Oelkers [43]. Furthermore, we hypothesize that phytoplankton might access limiting nutrients directly from the sediments within the microniches at the particle surfaces. The direct physical contact between phytoplankton or their extracted organic compounds might further reinforce the role of particulates as nutrient supplier and transport agent for organic carbon to the deep ocean. This,

however, needs further experimental and in-situ studies exploring the effect of riverine particulates on the growth of different types of phytoplankton and their mechanisms of nutrient uptake as well as the role of particulates in agglomeration and sedimentation of organic carbon.

The link between climate and riverine particulate transport is likely strongest during the end of glacial cycles, when glacial activity produces vast quantities of fine-grained material, transported to the oceans by glacial meltwater [43,112]. Furthermore, the transport of particulate material to the oceans during this time is likely facilitated through the influx of icebergs, which may transport nutrients to remote regions of the open ocean [120–123]. The increased supply of particulate material to the ocean likely increases primary productivity and organic carbon burial, thus contributing to drawing down atmospheric CO_2 levels and moderating global warming. As the CO_2 drawdown via the organic carbon cycle is concomitant with a rise in oxygen, produced during oxygenic photosynthesis, the enhanced organic carbon cycle towards the end of major glaciations may have played a major role in the atmospheric oxygenation events. The two major oxygenation events of the Earths' atmosphere occurred about 2.4-1.8 Ga ago (Great Oxidation Event (GOE, e.g. [124,125]) and during the Neoproterozoic, and both coincide with major "Snowball Earth" events, which occurred 2.4-2.1 Ga ago (Huronian glaciation, e.g. [126]) and during the Cryogenian period (Sturtian and Marionoan glaciations, ~0.7 Ga and ~0.65 Ga ago e.g. [127,128]). These major oxygenation and glaciation events furthermore coincide with carbon isotope excursions recorded in marine carbonates, which are interpreted as variations in organic matter burial [125,129]. Such observations suggest that the stabilization of the Earths' temperature through photosynthetic CO_2 drawdown and the oxygenation of the Earths' atmosphere through photosynthetic O_2 production may have been caused, at least in part, by particulate driven enhanced primary production and organic carbon burial.

5. Conclusions

The results obtained in this study demonstrate a positive effect of riverine particulate material on the growth of the marine diatom *Thalassiosira weissflogii*. In Guillard´s f/2 culture medium enriched Instant Ocean©, the presence of riverine particulates increased the total diatom concentration and slowed post-exponential net diatom death rates. In Instant Ocean© without additional nutrients, riverine particulates led to a linear increase in diatom concentrations as a function of particulate concentration, whereas diatom cultures died in controls without particulates. These results indicate a strong positive influence of riverine particulates on phytoplankton growth in coastal environments. Moreover, the presence of particulates is suggested to facilitate organic carbon burial through the delivery of surface area available for adsorption of organic compounds and through their role in the aggregation and sedimentation of phytoplankton. These combined effects suggest a major role of riverine particulates in the global carbon cycle, which becomes especially significant in view of the current major anthropogenic perturbations of global particle fluxes.

Data Availability Statement: The data presented in this study are partially available on request from the corresponding author.

Conflicts of Interest: The authors declare no conflict of interest.

References

1. Petit, J.R.; Jouzel, J.; Raynaud, D.; Barkov, N. I.; Barnola, J.-M.; Basile, I.; Bender, M.; Chappellaz, J.; Davis, M.; Delaygue, G.; Delmotte, M.; Kotlyakov, V. M.; Legrand, M.; Lipenkov, V.Y.; Lorius, C.; Pépin, L.; Ritz, C.; Saltzman, E.; Stievenard, M. Climate and atmospheric history of the past 420,000 years from the Vostok ice core, Antarctica. *Nature* **1999,** *399,* 429-436.

2. Oelkers, E.H.; Cole, D.R. Carbon Dioxide Sequestration A Solution to a Global Problem. *Elements* **2008,** *4,* 305–310.

3. IPCC 2018. Summary for Policymakers. In: Global warming of 1.5°C. An IPCC Special Report on the impacts of global warming of 1.5°C above pre-industrial levels and related global greenhouse gas emission pathways, in the context of strengthening the global response to the threat of climate change, sustainable development, and efforts to eradicate poverty [V. Masson-Delmotte; P. Zhai, H.O.; Pörtner, D.; Roberts, J., Skea, P. R. Shukla, A.; Pirani, W.; Moufouma-Okia, C., Péan, R., Pidcock, S., Connors, J.B.R.; Matthews, Y.; Chen, X.; Zhou, M.I.; Gomis, E.; Lonnoy, T.; Maycock, M.; Tignor, T.; Waterfield (eds.)]. 2018. World Meteorological Organization, Geneva, Switzerland, 32 pp.

4. Falkowski P.G.; Barber R.T.; Smetacek, V. Biogeochemical Controls and Feedbacks on Ocean Primary Production. *Science* **1998,** *281,* 200–206.

5. Falkowski, P.; Scholes, R.J.; Boyle, E.; Canadell, J.; Canfield, D.; et al. The Global Carbon Cycle. *Science* **2000,** *290,* 291–296.

6. Cavicchioli, R.; Ripple, W.J.; Timmis, K.N.; Bakken, L.R.; Baylis, M., et al. Scientists' warning to humanity: microorganisms and climate change. *Nat. Rev. Microbiol.* **2019,** *17,* 569–586.

7. Walker, J.C.; Hays, P.B.; Kasting, J.F. A negative feedback mechanism for the long-term stabilization of Earth's surface temperature. *J. Geophys. Res.-Oceans* **1981,** *86,* 9776–9782.

8. Berner, R.A. Burial of organic carbon and pyrite sulfur in the modern ocean: Its geochemical and environmental significance. *Am. J. Sci.* **1982,** *282,* 451–473.

9. Berner, R.A.; Lasaga, A.C.; Garrels R.M. The carbonate-silicate geochemical cycle and its effect on atmospheric carbon dioxide over the past 100 million years. *Am. J. Sci.* **1983,** *283,* 641–683.

10. Berner R.A.; Kothavala, Z. Geocarb III. *Am. J. Sci.* **2001,** *301,* 182–204.

11. Wallmann, K. Controls on the cretaceous and cenozoic evolution of seawater composition, atmospheric CO_2 and climate. *Geochim. Cosmochim. Acta* **2001,** *65,* 3005–3025.

12. Gislason, S.R.; Oelkers, E.H.; Eiriksdottir, E.S.; Kardjilov, M.I.; Gisladottir, G.; Sigfusson, B.; Snorrason, A.; Elefsen, S.; Hardardottir, J.; Torssander, P.; Oskarsson, N. Direct evidence of the feedback between climate and weathering. *Earth Planet. Sci. Lett.* **2009,** *277,* 213–222.

13. Labat, D.; Goddéris, Y.; Probst, J.L.; Guyot, J.L. Evidence for global runoff increase related to climate warming. *Adv. Water Resour.* **2004,** *27,* 631–642.

14. Gedney, N.; Cox, P.M.; Betts, R.A.; Boucher, O.; Huntingford, C.; Stott, P.A. Detection of a direct carbon dioxide effect in continental river runoff records. *Nature* **2006,** *439,* 835-838.

15. Gislason, S.R.; Oelkers, E.H.; Snorrason Á. Role of river-suspended material in the global carbon cycle. *Geology* **2006,** *34,* 49–52.

16. Hein, M.; Sand-Jensen K. CO_2 increases oceanic primary production. *Nature* **1997,** *388,* 526-527.

17. Clark, D.R.; Flynn K.J. The relationship between the dissolved inorganic carbon concentration and growth rate in marine phytoplankton. *P. Roy. Soc. Lond. B Bio.* **2000,** *267,* 953–959.

18. Riebesell, U.; Zondervan, I.; Rost, B.; Tortell, P.D.; Zeebe, R.E.; Morel F.M. Reduced calcification of marine plankton in response to increased atmospheric CO_2. *Nature* **2000,** *407,* 364-367.

19. Tortell, P.D.; DiTullio, G.R.; Sigman, D.M.; Morel F.M. CO_2 effects on taxonomic composition and nutrient utilization in an Equatorial Pacific phytoplankton assemblage. *Mar. Ecol. Prog. Ser.* **2002,** *236,* 37–43.

20. Riebesell, U.; Schulz, K.G.; Bellerby, R.G.; Botros, M.; Fritsche, P.; Meyerhöfer, M.; Neill, C.; Nondal, G.; Oschlies, A.; Wohlers, J.; Zöllner, E. Enhanced biological carbon consumption in a high CO_2 ocean. *Nature* **2007,** *450,* 545-548.

21. Rost, B.; Zondervan, I.; Wolf-Gladrow, D. Sensitivity of phytoplankton to future changes in ocean carbonate chemistry. *Mar. Ecol. Prog. Ser.* **2008,** *373,* 227–238.

22. Feng, Y.; Hare, C.E.; Leblanc, K.; Rose, J.M.; Zhang, Y.; DiTullio, G.R. ; et al. Effects of increased pCO$_2$ and temperature on the North Atlantic spring bloom. I. The phytoplankton community and biogeochemical response. *Mar. Ecol. Prog. Ser.* **2009,** *388,* 13–25.

23. Passow, U.; Carlson, C.A. The biological pump in a high CO$_2$ world. *Mar. Ecol. Prog. Ser.*   **2012,** *470,* 249–271.

24. Engel, A.; Borchard, C.; Piontek, J.; Schulz, K.G.; Riebesell, U.; Bellerby, R. CO$_2$ increases ^{14}C primary production in an Arctic plankton community. *Biogeosciences* **2013,** *10,* 1291–1308.

25. Boyd, P.W. Toward quantifying the response of the oceans' biological pump to climate change. *Front. Mar. Sci.* **2015,** *13,* 77.

26. Arrigo, K.R. Carbon cycle: Marine manipulations. *Nature* **2007,** *450,* 491-492.

27. Passow, U.; Laws E.A. Ocean acidification as one of multiple stressors. *Mar. Ecol. Prog. Ser.* **2015,** *541,* 75–90.

28. Seebah, S.; Fairfield, C.; Ullrich, M.S.; Passow, U. Aggregation and Sedimentation of *Thalassiosira weissflogii* (diatom) in a Warmer and More Acidified Future Ocean. *PLOS ONE* **2014,** *9,* e112379.

29. Frogner, P.; Gíslason, S.R.; Óskarsson, N. Fertilizing potential of volcanic ash in ocean surface water. *Geology* **2001,** *29,* 487–490.

30. Jickells, T.D.; An, Z.S.; Andersen, K.K.; Baker, A.R.; Bergametti, G.; et al. Global Iron Connections Between Desert Dust, Ocean Biogeochemistry, and Climate. *Science* **2005,** *308,* 67–71.

31. Jones, M.T.; Gislason, S.R. Rapid releases of metal salts and nutrients following the deposition of volcanic ash into aqueous environments. *Geochim. Cosmochim. Acta* **2008,** *72,* 3661–3680.

32. Olsson, J.; Stipp, S.L.S.; Dalby, K.N.; Gislason, S.R. Rapid release of metal salts and nutrients from the 2011 Grímsvötn, Iceland volcanic ash. *Geochim. Cosmochim. Acta* **2013,** *123,* 134–149.

33. Eiriksdottir, E.S.; Gislason, S.R.; Oelkers, E.H. Direct evidence of the feedback between climate and nutrient, major, and trace element transport to the oceans. *Geochim. Cosmochim. Acta* **2015,** *166,* 249–266.

34. Eiriksdottir, E.S.; Oelkers, E.H.; Hardardottir, J.; Gislason, S.R. The impact of damming on riverine fluxes to the ocean. *Water Res.* **2017,** *113,* 124–138.

35. Gaillardet, J.; Dupré, B.; Allègre, C.J. Geochemistry of large river suspended sediments. *Geochim. Cosmochim. Acta* **1999,** *63,* 4037–4051.

36. Gaillardet, J.; Viers, J.; Dupré, B. Chapter 5.09 - Trace Elements in River Waters. In Treatise on Geochemistry (eds. H. D. Holland and K. K. Turekian). Pergamon. Oxford, **2003,** pp. 225–272.

37. Meybeck, M.; Laroche, L.; Dürr, H.H.; Syvitski, J.P.M. Global variability of daily total suspended solids and their fluxes in rivers. *Global Planet. Change* **2003,** *39,* 65–93.

38. Syvitski, J.P.M.; Peckham, S.D.; Hilberman, R.; Mulder, T. Predicting the terrestrial flux of sediment to the global ocean: A planetary perspective. *Sediment. Geol.* **2003,** *162,* 5–24.

39. Walling D.E. Human impact on land–ocean sediment transfer by the world's rivers. *Geomorphology* **2006,** *79,* 192–216.

40. Viers, J.; Dupré, B.; Gaillardet, J. Chemical composition of suspended sediments in World Rivers. *Sci. Total Environ.* **2009,** *407,* 853–868.

41. Oelkers, E.H.; Gislason, S.R.; Eiriksdottir, E.S.; Jones, M.; Pearce, C.R.; Jeandel, C. The role of riverine particulate material on the global cycles of the elements. *Appl. Geochem.* **2011,** *26,* S365-S369.

42. Oelkers, E.H.; Jones, M.T.; Pearce, C.R.; Jeandel, C.; Eiriksdottir, E.S.; Gislason, S.R. Riverine particulate material dissolution in seawater and its implications for the global cycles of the elements. *C. R. Geosci.* **2012,** *344,* 646–651.

43. Jeandel, C.; Oelkers, E.H. The influence of terrigenous particulate material dissolution on ocean chemistry and global element cycles. *Chem. Geol.* **2015,** *395,* 50–66.

44. De La Rocha, C.L.; Passow, U. Recovery of *Thalassiosira weissflogii* from nitrogen and silicon starvation. *Limnol. Oceanogr.* **2004,** *49,* 245–255.

45. Field, C.B.; Behrenfeld, M.J.; Randerson, J.T; Falkowski, P. Primary Production of the Biosphere. *Science* **1998,** *281,* 237–240.

46. Armbrust, E. The life of diatoms in the world's oceans. *Nature* **2009,** *459,* 185–192.

47. Malviya, S.; Scalco, E.; Audic, S.; Vincent, F.; Veluchay, A.; Poulain, J.; Wincker, P.; Lucicone, D.; de Vargas, C.; Bittner, L.; Zingone, A.; Bowler, C. Insights into global distribution and diversity in the worlds ocean. *Proc. Nat. Acad. Sci.* **2016,** *113,* E1516-E1525.

48. Gao, K.; Campbell, D.A. Photophysiological responses of marine diatoms to elevated CO_2 and decreased pH: a review. *Functional Plant Biology* **2014,** *41,* 449-459.

49. Tréguer, P.; Bowler, C.; Moriceau, B.; Dutkiewicz, S.; Gehlen, M.; Aumont, O.; Bittner, L.; Dugdale, R.; Finkel, Z.; Ludicone, D.; Jahn, O.; Guidi, L.; Lasblei, M.; Leblanc K.; Levy, M.; Pomndaven, P. Influence of diatom diversity on the ocean biological carbon pump. *Nature Geosci.* **2018,** *11,* 27–37.

50. Bach, L.T.; Taucher, J. CO_2 effects on diatoms: a synthesis of more than a decade of ocean acidification experiments with natural communities. *Ocean Sci.* **2019,** *15,* 1159–1175.

51. Petrou, K.; Baker, K.G.; Nielsen, D.A.; Hancock, A.M.; Schulz, K.G.; Davidson, A.T. Acidification diminishes diatom silica production in the Southern Ocean. *Nat. Clim. Chang.* **2019,** *9,* 781–786.

52. Edwards, M.; Beaugrand, G.; Kléparski, L.; Helaouet, P.; Reid, P.C. Climate variability and multi-decadal diatom abundance in the Northeast Atlantic. *Commun Earth Environ.* **2022,** *3,* 162.

53. Taucher, J.; Bach, L.T.; Prowe, A.E.F.; Boxhammer, T.; Kvale, K.; Riebesell, U. Enhanced silica export in a future ocean triggers global diatom decline. *Nature* **2022,** *605,* 696–700.

54. Boyd, P.W.; Claustre, H.; Levy, M.; Siegel, D.A.; Weber, T. Multi-faceted particle pumps drive carbon sequestration in the ocean. *Nature* **2019,** *568,* 327–335.

55. Le Moigne, F.A.C. Pathways of organic carbon downward transport by the ocean biological carbon pump. *Front. Mar. Sci.* **2019,** *6,* 634.

56. Jackson, G.A.; Lochmann, S.E. Effect of coagulation on nutrient and light limitation of an algal bloom. *Limnol. Oceanogr.* **1992,** *37,* 77–89.

57. Alldredge, A.L.; Gotschalk, C.; Passow, U.; Riebesell, U. Mass aggregation of diatom blooms. *Deep-Sea Res. Pt II* **1995,** *42,* 9–27.

58. Alldredge, A.L.; Jackson G.A. Preface: Aggregation in marine system. *Deep-Sea Res. Pt II* **1995,** *42,* 1–7.

59. Laufkötter, C.; Vogt, M.; Gruber, N.; Aumont, O.; Bopp, L.; Doney, S.C.; Dunne, J.P.; Hauck, J.; John, J.G.; Lima, I.D.; Seferian, R.; Völker, C. Projected decreases in future marine export production: the role of the carbon flux through the upper ocean ecosystem. *Biogeosciences* **2016,** *13,* 4023–4047.

60. McCave, I.N. Size spectra and aggregation of suspended particles in the deep ocean. *Deep-Sea Res.* **1984,** *31,* 329–352.

61. Smetacek, V.S. Role of sinking in diatom life-history cycles: Ecological, evolutionary and geological significance. *Mar. Biol.* **1985,** *84,* 239–251.

62. Hill, P.S. Reconciling aggregation theory with observed vertical fluxes following phytoplankton blooms. *J. Geophys. Res.-Oceans* **1992,** *97,* 2295–2308.

63. Jackson, G.A. A model of the formation of marine algal flocs by physical coagulation processes. *Deep-Sea Res.* **1990,** *37,* 1197–1211.

64. Avnimelech, Y.; Troeger, B.W.; Reed, L.W. Mutual Flocculation of Algae and Clay. *Science* **1982,** *216,* 63.

65. Ding, X.; Henrichs, S.M. Adsorption and desorption of proteins and polyamino acids by clay minerals and marine sediments. *Mar. Chem.* **2002,** *77,* 225–237.

66. Beaulieu, S.E.; Sengco, M.R.; Anderson, D.M. Using clay to control harmful algal blooms. *Harmful Algae* **2005,** *4,* 123–138.

67. Verspagen, J.M.; Visser, P.M.; Huisman, J. Aggregation with clay causes sedimentation of the buoyant cyanobacteria *Microcystis* spp. *Aquat. Microb. Ecol.* **2006,** *44,* 165–174.

68. Passow, U.; De La Rocha, C.; Fairfield, C.; Schmidt, K. Aggregation as a function of and mineral particles. *Limnol. Oceanogr.* **2014,** *59,* 532–547.

69. Ploug, H.; Iversen, M.H.; Fischer, G. Ballast, sinking velocity, and apparent diffusivity within marine snow and zooplankton fecal pellets: Implications for substrate turnover by attached bacteria. *Limnol. Oceanogr.* **2008,** *53,* 1878–1886.

70. Ploug, H.; Iversen, M.H.; Koski, M.; Buitenhuis, E.T. (2008b) Production, oxygen respiration rates, and sinking velocity of copepod fecal pellets: Direct measurements of ballasting by opal and calcite. *Limnol. Oceanogr.* **2008,** *53,* 469–476.

71. Passow, U.; De La Rocha, C.L. Accumulation of mineral ballast on organic aggregates. *Global Biogeochem. Cycles* **2006,** *20,* GB1013.

72. De La Rocha, C.L.; Passow, U. Factors influencing the sinking of POC and the efficiency of the biological carbon pump. *Deep-Sea Res. Pt II* **2007,** *54,* 639–658.

73. Liu, H.; Yuan, P.; Liu, D.; Zhang, W.; Tian Q.; Bu, H.; Wei, Y.; Xia, J.; Wang, Y.; Zhou, J. Insight into cyanobacterial preservation in shallow marine environments from experimental simulation of cyanobacteria-clay co-aggregation. *Chem. Geol.* **2021,** *577,* 120285.

74. Smetacek, V. Biological oceanography: Diatoms and the silicate factor. *Nature* **1998,** *391,* 224-225.

75. Tréguer, P.; Pondaven, P. Silica control of carbon dioxide. *Nature* **2000,** *406,* 338-359.

76. Mayer, L.M. Surface area control of organic carbon accumulation in continental shelf sediments. *Geochim. Cosmochim.* Acta **1994,** *58,* 1271–1284.

77. Lalonde, K.; Mucci, A.; Ouellet, A.; Gélinas, Y. Preservation of organic matter in sediments promoted by iron. *Nature* **2012,** *483,* 198-200.

78. Eiriksdottir, E.S.; Louvat, P.; Gislason, S.R.; Óskarsson, N.; Hardardóttir, J. Temporal variation of chemical and mechanical weathering in NE Iceland. *Earth Planet. Sci. Lett.* **2008,** *272,* 78–88.

79. Milliman, J.D.; Syvitski, J.P. Geomorphic/Tectonic Control of Sediment Discharge to the Ocean. *J. Geol.* **1992,** *100,* 525–544.

80. Guillard, R.R. Culture of Phytoplankton for Feeding Marine Invertebrates. In Culture of Marine Invertebrate Animals: Proceedings — 1st Conference on Culture of Marine Invertebrate Animals Greenport (eds. W. L. Smith and M. H. Chanley). Springer US. Boston, MA, **1975,** pp. 29–60.

81. Johansen, J.R.; Theriot, E. The relationship between valve diameter and number of central flutoportulae in *Thalassiosira weissflogii* (Barcillariophyceae). *J. Phycol.* **1987,** *23,* 663–665.

82. Atkinson, M.J.; Barnett, H.; Aceves, H.; Langdon, C.; Carpenter, S.J.; McConnaughey, T.; Hochberg, E.; Smith, M.; Marino, B.D.V. The Biosphere 2 coral reef biome. *Ecol. Eng.* **1999,** *13,* 147–172.

83. Roberts, S.B.; Lane, T.W.; Morel, F.M. Carbonic anhydrase in the marine diatom *Thalassiosira weissflogii* (Barcillariophyceae). *J. Phycol.* **1997,** *33,* 845–850.

84. De La Rocha, C.L.; Terbrüggen, A.; Völker, C.; Hohn, S. Response to and recovery from nitrogen and silicon starvation in *Thalassiosira weissflogii*: growth rates, nutrient uptake and C, Si and N content per cell. *Mar. Ecol. Prog. Ser.* **2010,** *412,* 57–68.

85. Sorhannus, U.; Ortiz, J.D.; Wolf, M.; Fox, M.G. Microevolution and Speciation in *Thalassiosira weissflogii* (Bacillariophyta). *Protist* **2010,** *161,* 237–249.

86. Vella, F.M.; Sardo, A.; Gallo, C.; Landi, S.; Fontana, A.; d'Ippolito, G. Annual outdoor cultivation of the diatom *Thalassiosira weissflogii*: productivity, limits and perspectives. *Algal Research* **2019,** *42,* 101553.

87. Ernst, A.; Deicher, M.; Herman, P.M.; Wollenzien, U.I. Nitrate and Phosphate Affect Cultivability of Cyanobacteria from Environments with Low Nutrient Levels. *Appl. Environ. Microb.* **2005,** *71,* 3379–3383.

88. Waite, A.; Fisher, A.; Thompson, P.A.; Harrison, P.J. Sinking rate versus cell volume relationships illuminate sinking rate control mechanisms in marine diatoms. *Mar. Ecol. Prog. Ser.* **1997,** *157,* 97–108.

89. Brady, P.V; Walther, J.V. Kinetics of quartz dissolution at low temperatures. *Chem. Geol.* **1990,** *82,* 253–264.

90. Gislason, S.R.; Oelkers, E.H. Mechanism, rates, and consequences of basaltic glass dissolution. *Geochim. Cosmochim. Acta* **2003,** *67,* 3817–3832.

91. Gélabert, A.; Pokrovsky, O.S.; Schott, J.; Boudou, A.; Feurtet-Mazel, A. Cadmium and lead interaction with diatom surfaces: A combined thermodynamic and kinetic approach. *Geochim. Cosmochim. Acta* **2007,** *71,* 3698–3716.

92. Poulton, S.W.; Raiswell, R. Chemical and physical characteristics of iron oxides in riverine and glacial meltwater sediments. *Chem. Geol.* **2005,** *218,* 203–221.

93. Palenik, B.; Morel, F.M.M. Comparison of cell-surface L-amino acid oxidases from several marine phytoplankton. *Mar. Ecol. Progr. Ser.* **1990,** *59,* 195-201.

94. Cermeno, P.; Falkowski, P.G.; Romero, O.E.; Schaller, M.F.; Vallina, S. M. Continental erosion and the Cenozoic rise of marine diatoms. *Proc. Nat. Acad. Sci.* **2015,** *112,* 4239-4244.

95. Gordeev, V.V.; Martin, J.M.; Sidorov, I.S.; Sidorova, M. A reassessment of the Eurasian river input of water, sediment, major elements, and nutrients to the Arctic Ocean. *Am. J. Sci.* **1996,** *296,* 664–691.

96. Pokrovsky, O.S.; Viers, J.; Dupré, B.; Chabaux, F.; Gaillardet, J.; Audry, S.; Prokushkin, A.S.; Shirokova, L. S.; Kirpotin, S.N.; Lapitsky, S.A.; Shevchenko, V.P. Biogeochemistry of carbon, major and trace elements in watersheds of northern Eurasia: The change of fluxes, sources and mechanisms under the climate warming prospectivedrained to the Arctic Ocean. *C. R. Geosci.* **2012,** *344,* 663–677.

97. Gordeev, V.V.; Dara, O.M.; Filippov, A.S.; Belorukov, S.K.; Lokhov, A.S.; Kotova, E.I.; Kochenkova, A.I. Mineralogy of Particulate Suspended Matter of the Severnaya Dvina River (White Sea, Russia). *Minerals* **2022,** *12,* 1600. https://doi.org/10.3390/min12121600.

98.   Baisre, J.A.; Arboleya, Z. Going against the flow. *Fish. Res.* **2006,** *81,* 283–292.

99.   Jones, J.I.; Duerdoth, C.P.; Collins, A.L.; Naden, P.S.; Sear, D.A. Interactions between diatoms and fine sediment. *Hydrol. Processes* **2012,** *28,* 1226-1237.

100. Jiang, Z.; Liu, J.; Chen, J.; Chen, Q.; Yan, X.; Xuan, J.; Zeng, J. Responses of summer phytoplankton community to drastic environmental changes in the Changjiang (Yangtze River) estuary during the past 50 years. *Water Res.* **2014,** *54,* 1–11.

101. Chen, C.; Mao, Z.; Tang, F.; Han, G.; Jiang, Y. Declining riverine sediment input impact on spring phytoplankton bloom off the Yangtze River Estuary from 17-year satellite observation. *Cont. Shelf. Res.* **2017,** *135,* 86–91.

102. Burd, A.B.; Jackson, G.A. Particle Aggregation. *Ann. Rev. Marine Sci.* **2009,** *1,* 65-90.

103. Richardson, T.L. Mechanisms and pathways of small-phytoplankton export from the surface ocean. *Ann. Rev. Marine Sci.* **2019,** *11,* 57-74.

104. Rixen, T.; Gaye, B.; Eeis, K.-C.; Ramasway, V. The ballast effect of lithogenic matter and its influences on the carbon fluxes in the Indian Ocean. *Biosciences* **2019,** *16,* 486-503.

105. Armstrong, R.A.; Lee, C.; Hedges, J.I.; Honjo, S.; Wakeham S. G. A new, mechanistic model for organic carbon fluxes in the ocean based on the quantitative association of POC with ballast minerals. *Deep-Sea Res. Pt II* **2001,** *49,* 219–236.

106. Iversen, M.H.; Robert, M.L. Ballasting effects of smectite on aggregate formation and export from a natural plankton community. *Mar. Chem.* **2015,** *175,* 18-27.

107. Anderson, M.A.; Morel F.M. The influence of aqueous iron chemistry on the uptake of iron by the coastal diatom *Thalassiosira weissflogii. Limnol. Oceanogr.* **1982,** *27,* 789–813.

108. Milligan, A.J.; Mioni, C.E.; Morel, F.M.M. Response of cell surface pH to pCO_2 and iron limitation in the marine diatom *Thalassiosira weissflogii. Mar. Chem.* **2009,** *114,* 31–36.

109. Wolf-Gladrow, D.; Riebesell, U. Diffusion and reactions in the vicinity of plankton: A refined model for inorganic carbon transport. *Mar. Chem.* **1997,** *59,* 17–34.

110. Shaked, Y.; Kustka, A.B.; Morel, F.M. A general kinetic model for iron acquisition by eukaryotic phytoplankton. *Limnol. Oceanogr.* **2005,** *50,* 872–882.

111. Rogers, J.R.; Bennett, P.C.; Choi, W.J. Feldspars as a source of nutrients for microorganisms. *Am. Mineral.* **1998,** *83,* 1532–1540.

112. Rogers, J.R.; Bennett, P.C. Mineral stimulation of subsurface microorganisms: Release of limiting nutrients from silicates. *Chem. Geol.* **2004,** *203,* 91–108.

113. Bailey, B.; Templeton, A.; Staudigel, H.; Tebo, B.M. Utilization of Substrate Components during Basaltic Glass Colonization by Pseudomonas and Shewanella Isolates. *Geomicrobiol. J.* **2009,** *26,* 648–656.

114. Sudek, L.A.; Wanger, G.; Templeton, A.S.; Staudigel, H.; Tebo, B.M. Submarine Basaltic Glass Colonization by the Heterotrophic Fe(II)-Oxidizing and Siderophore-Producing Deep-Sea Bacterium *Pseudomonas stutzeri* VS-10: The Potential Role of Basalt in Enhancing Growth. *Front. Microbiol.* **2017,** *8,* 363.

115. Mayer, L.M.; Keil, R.G.; Macko, S.A.; Joye, S.B.; Ruttenberg, K.C.;   Aller, R.C. Importance of suspended participates in riverine delivery of bioavailable nitrogen to coastal zones. *Global Biogeochem. Cycles* **1998,** *12*(4), 573-570. https://doi.org/10.1029/98GB02267.

116. Jones, M.T.; Pearce, C.R.; Oelkers, E.H. An experimental study of basaltic riverine particulate material and seawater. *Geochim. Cosmochim. Acta* **2011,** *77,* 108-120.

117. Jones, M.T.; Pearce, C.R.; Jeandel, C.; Gislason, S.R.; Eiriksdottir E.; Mavromatis V.; Oelkers, E.H. Riverine particulate material dissolution as a significant flux of strontium to the oceans. *Earth Planet. Science Lett.* **2012,** *355,* 51-59.

118. Jones, M.T.; Gislason, S.R.; Burton, K.W.; Pearce, C.R.; Mavromatis V.; Pogge Van Strandmann, P.A.E.; Oelkers, E.H. Quantifying the impact of riverine particulate dissolution in seawater on ocean chemistry. *Earth Planet. Sci. Lett.* **2014,** *395,* 91-100.

119. Alley, R.B.; Cuffey, K.M.; Evenson, E.B.; Strasser, J.C.; Lawson, D.E.; Larson, G.J. How glaciers entrain and transport basal sediment. *Quaternary Sci. Rev.* **1997,** *16,* 1017–1038.

120. Broecker, W.S. Massive iceberg discharges as triggers for global climate change. *Nature* **1994,** *372,* 421-424.

121. Hemming, S.R. Heinrich events: Massive late Pleistocene detritus layers of the North Atlantic and their global climate imprint. *Rev. Geophys.* **2004,** *42,* RG1005.

24

122. Raiswell, R.; Hawkings, J.R.; Benning, L.G.; Baker, A.R.; Death, R.; Albani, S.; Mahowald, N.; Krom, M. D.; Poulton, S.W.; Wadham, J.; Tranter, M. Potentially bioavailable iron delivery by iceberg-hosted sediments and atmospheric dust to the polar oceans. *Biogeosciences* **2016,** *13,* 3887–3900.

123. Hawkings, J.R.; Wadham, J.L.; Benning, L.G.; Hendry, K.R.; Tranter, M.; Tedstone, A.; Nienow, P.; Raiswell, R. Ice sheets as a missing source of silica to the polar oceans. *Nat. Commun.* **2017,** *8,* 14198.

124. Holland, H.D. Volcanic gases, black smokers, and the great oxidation event. *Geochim. Cosmochim. Acta* **2002,** *66,* 3811–3826.

125. Shields-Zhou, G.; Och, L. The case for a Neoproterozoic Oxygenation Event. *GSAT* **2011,** *21,* 4–11.

126. Tang, H.; Chen, Y. Global glaciations and atmospheric change at ca. 2.3 Ga. *Geosci. Front.* **2013,** *4,* 583–596.

127. Arnaud, E.; Halverson, G.P.; Shields-Zhou, G. The geological record of Neoproterozoic ice ages, Chapter 1. *Geol. Soc., London, Mem.* **2011,** *36,* 1–16.

128. Rooney, A.D.; Strauss, J.V.; Brandon, A.D.; Macdonald, F.A. A Cryogenian chronology: Two long-lasting synchronous Neoproterozoic glaciations. *Geology* **2015,** *43,* 459–462.

129. Holland, H.D. The oxygenation of the atmosphere and oceans. *Philos. T. Roy. Soc. B Bio.* **2006,** *361,* 903–915.